DOI: 10.1021/ma101324j

Macromolecules
ARTICLE

Sedimentation of Polyelectrolyte Chains in Aqueous Solutions

Zhenli Luo[†] and Guangzhao Zhang*[,†,‡]

[†]*Hefei National Laboratory for Physical Sciences at Microscale, Department of Chemical Physics, University of Science and Technology of China, Hefei, P. R. China 230026, and*
[‡]*Faculty of Materials Science and Engineering, South China University of Technology, Guangzhou, P. R. China 510640*

Received June 15, 2010; Revised Manuscript Received November 3, 2010

ABSTRACT: We have investigated the dynamics of poly(sodium styrenesulfonate) (PSSNa) in aqueous solutions with and without added salt (NaCl) by use of analytical ultracentrifuge (AUC) via sedimentation velocity (SV) as a function of NaCl concentration (C_s) or PSSNa concentration (C_p). As C_s increases, the sedimentation coefficient monotonically increases, whereas the diffusion coefficient shows a minimum. On the other hand, as C_p increases, the sedimentation coefficient decreases while the diffusion coefficient exhibits a minimum at $C_s < 1.0 \times 10^{-3}$ M. However, they linearly vary with C_p at $C_s > 1.0 \times 10^{-3}$ M. The scaling relation between the molar mass and sedimentation coefficient or diffusion coefficient at infinite dilution indicates that PSSNa chain changes from an extended conformation to a random coil as NaCl concentration increases. Our experiments demonstrate that the dynamics of polyelectrolyte chains is mediated by interchain electrostatic repulsion, hydrodynamic interactions, and intrinsic excluded volume effect.

Introduction

Polyelectrolytes are highly charged macromolecules which dissociate into charged backbone and small counterions in aqueous solution or polar organic solvents. Biological macromolecules such as proteins, DNA, and RNA are polyelectrolytes. Many synthetic polyelectrolytes have found applications in flocculants, dispersants, water softeners, drug delivery, and other fields.[1] It is recognized that the behaviors and properties of polyelectrolytes are determined by the electrostatic interactions which are mediated by ionic strength, counterion valence, solvent quality, polyelectrolyte concentration, and the charge density in polyelectrolyte chains.[2−4] Yet, how the electrostatic interactions work is not well understood.

Theoretically, the Manning−Oosawa counterion condensation[5,6] has been the fundamental to understand polyelectrolyte behaviors. Generally, the counterion condensation induced by the electrostatic attraction between polyelectrolyte chains and small counterions reduces the effective charges on polyelectrolyte chains and weakens the electrostatic interaction between polyelectrolyte chains.[5−8] Odijk,[9] Skolnick, and Fixman[10,11] demonstrated that the unscreened Coulomb interactions lead to highly induced stiffness, and the electrostatic persistence length is proportional to the square of the Debye length. In a salt-free solution, electrostatic repulsion between polyelectrolyte chains is strong due to the weak counterion condensation, so that linear polyelectrolyte chains are highly extended. As the added salt concentration increases, the Debye screening length decreases, and the electrostatic interaction is gradually screened. Consequently, the polyelectrolyte chains become more flexible. Experimentally, polyelectrolyte solutions have been studied by viscometry,[12,13] small-angle neutron scattering,[14,15] and light scattering.[16−19] Previous studies revealed polyelectrolyte behavior is determined by the interplay between hydrodynamic interactions, intrinsic excluded volume effect, and the electrostatic interactions.[12,20−24] Yet, the behavior of polyelectrolyte solutions is very complicated because it is a many-body problem. So far, many questions are still open.

Analytical ultracentrifuge (AUC) has been used to measure the molecular parameters of polymers via sedimentation equilibrium (SE) and sedimentation velocity (SV) analyses for decades.[25,26] The former can measure the molar mass, virial coefficient, and osmotic coefficient,[27−29] whereas the latter gives the information about the chain conformation of polymers via sedimentation coefficient and diffusion coefficient.[30−35] However, traditional SV data analysis cannot distinguish the diffusion from the solute polydispersity,[36] which limits its applications. Recently, a newly developed analysis provides a numerical solution of SV data so that the diffusion coefficient can be obtained from SV measurements besides the sedimentation coefficient.[37,38] Moreover, the molar mass can be determined based on the Svedberg equation with the data. In the present work, we have studied the sedimentation of poly(sodium styrenesulfonate) (PSSNa) with different molar mass in aqueous solutions with and without added salt by use of such a AUC technique. Our aim is to understand the effect of molecular interactions on the dynamics of polyelectrolyte chains.

Experimental Section

Sample Preparation. Sodium chloride (NaCl) (99.5%, Sinopharm Chemical Reagent), sodium hydroxide (NaOH) (95%, Sinopharm Chemical Reagent), were used as received. Poly(styrenesulfonic acid) (PSSH) samples (Polymer Source) are highly sulfonated polystyrenes. PSSNa was prepared by titrating PSSH using excessive NaOH solution. The products were dialyzed by Milli-Q water (Millipore, resistivity = 18.2 MΩ·cm, 25 °C) for 5 days and freeze-dried. The weight-average molar mass (M_w) of each PSSNa sample was measured by SV and SE analysis. The polydispersity index (PDI) was estimated by SV analysis. The characterization data are summarized in Table 1. PSSNa solution with concentration of 2.0 mg/mL and NaCl solution with concentration of 1.0 M were prepared as stock solutions for experiments.

SE Measurements. SE measurements were conducted on a Beckman Optima XL-I analytical ultracentrifuge (Beckman

*To whom correspondence should be addressed. E-mail: gzzhang@ustc.edu.cn.

 Published on Web 11/17/2010

Table 1. Characterization Data of PSSNa Samples

sample	sulfonation degree[a] (%)	M_w[b]/(10^3 g/mol)	M_w[c]/(10^3 g/mol)	PDI[c]	PDI[d]
PSSNa1	80.0	12.5	12.1	1.12	1.05
PSSNa2	70.6	34.6	32.3	1.07	1.03
PSSNa3	78.8	44.7	41.4	1.12	1.03
PSSNa4	92.3	82.9	80.1	1.15	1.05
PSSNa5	84.9	128.9	128.0	1.22	1.05
PSSNa6	87.7	572.0	621.4	2.15	1.09

[a] Estimated from the sulfur content by elemental analysis. [b] Determined by SE analysis at 0.1 M NaCl. [c] Determined by SV analysis at 0.1 M NaCl. [d] PDI values of the polystyrene precursors determined by size exclusion chromatography provided by manufacturer.

Coulter Instruments) at 20 °C. UV−vis absorption optics was used as detector. Three cells assembled by sapphire windows and six-sector 12 mm length Epon centerpieces were loaded to an An-60 Ti rotor. PSSNa samples with concentrations (C_p) of 0.050, 0.10, and 0.20 mg/mL in 0.10 M NaCl aqueous solution were measured at 260 nm with proper rotation speeds, and the molar mass was determined based on eq 1

$$c = c_0 \exp\left(\frac{M_w(1-\nu\rho_0)}{RT}\omega^2\frac{r^2-r_0^2}{2}\right) \quad (1)$$

where M_w, ν, ρ_0, R, T, and ω are the solute molar mass, partial specific volume, solvent density, gas constant, absolute temperature, and angular velocity, respectively. r is the radial distance from the rotation axis and c the solute concentration; r_0 and c_0 are radial distance and solute concentration at reference position, respectively.[25] ν was determined on an Anton Paar DMA 4500 densitometer. Our experiments revealed that ν has dependence on NaCl concentration but not on molar mass of PSSNa. As NaCl concentration increases from 0 to 0.5 M, ν increases from 0.555 ± 0.005 to 0.590 ± 0.016 mL/g. The SE data were analyzed by SEDPHAT (version 6.5).[38] The SE analysis determines molar mass with a relative error of 2%.[39] The results are summarized in Table 1, and a typical SE analysis profile can be found in the Supporting Information.

SV Measurements. SV experiments were performed on the same AUC at 20 °C with a rotation speed of 60 000 rpm. Cells were assembled by quartz or sapphire windows and two-sector 12 mm length Epon centerpieces. A volume of 400 μL of PSSNa solution and a volume of 420 μL of Milli-Q water as the reference were loaded. UV−vis absorption optics was used as detector. NaCl concentrations (C_s) used were 0−0.50 M. PSSNa concentrations (C_p) used were 0.0015−1.0 mg/mL and 0.10−1.0 mg/mL when C_s is below and above 3.0×10^{-4} M, respectively. We estimated the overlap concentration (C^*) of each PSSNa solution from the viscosity data in previous studies.[40,41] Each PSSNa solution has a concentration below C^*, except the highest molar mass sample (PSSNa6) in salt-free and low salt solution, whose concentration is close to C^*. For each sample, 50−200 scans of data were acquired at a time interval of 3 min at wavelength from 225 to 275 nm to ensure the absorbance lower than 1. The sedimentation process can be described by the Lamm equation[26]

$$\frac{\partial c}{\partial t} = D\left[\frac{\partial^2 c}{\partial r^2} + \frac{1}{r}\frac{\partial c}{\partial r}\right] - s\omega^2\left[r\frac{\partial c}{\partial r} + 2c\right] \quad (2)$$

where t, D, and s are the sedimentation time, diffusion coefficient, and sedimentation coefficient in units of svedberg (Sv) or 10^{-13} s, respectively. The sedimentation coefficient is defined as[26]

$$s = \frac{u}{\omega^2 r} = \frac{\mathrm{d}\ln r}{\omega^2\,\mathrm{d}t} \quad (3)$$

where u is the sedimentation velocity of the solute. s relates to D by the Svedberg equation, and hydrodynamic radius (R_h) relates to D by the Stokes−Einstein equation[26]

$$M = \frac{RT}{(1-\nu\rho_0)}\frac{s}{D} \quad (4)$$

$$D = \frac{k_B T}{f} = \frac{k_B T}{6\pi\eta R_h} \quad (5)$$

where k_B, f, and η are the Boltzmann constant, frictional ratio, and solvent viscosity, respectively. ρ_0 and η were calculated by the SEDNTERP program.[42]

For solute sedimentation in different solvents, the sedimentation coefficient is usually converted to standard condition ($s_{20,w}$) based on eq 6 to eliminate the effect of solvent viscosity.[26]

$$s_{20,w} = s_{20,exp}\left(\frac{\eta_{20,s}}{\eta_{20,w}}\right)\frac{1-\nu\rho_{20,w}}{1-\nu\rho_{20,s}} \quad (6)$$

where the $s_{20,exp}$ and $s_{20,w}$ are experimental sedimentation coefficient and standard sedimentation coefficient in water at 20 °C. $\eta_{20,s}$ and $\eta_{20,w}$ are viscosity of solvent and water at 20 °C. $\rho_{20,s}$ and $\rho_{20,w}$ are density of solvent and water at 20 °C, respectively. In the present study, the sedimentation coefficient was converted to standard sedimentation coefficient ($s_{20,w}$) and written as s for convenience.

Results and Discussion

Data Analysis. SEDFIT (version 11.71) developed by Schuck[37] was adopted to analyze the data, where the continuous $c(s)$ distribution model with maximum entropy or second derivative regularization is used to fit s, D, and M_w. Our preliminary experiments showed that they did not make a difference in the fitting for the present systems. Here, we only present the data from the former.

Strictly, the continuous $c(s)$ distribution model is only for rigid spheres.[43] A distorted diffusion coefficient distribution is obtained for linear macromolecules. To test the applicability of SEDFIT for polyelectrolytes, we also determined the sedimentation coefficients of PSSNa by the Transport model (XL-I Data Analysis software, version 6.04) based eq 3. It shows that the sedimentation coefficients determined by the two models agree with each other (see Supporting Information). The results are also generally consistent with those in a previous AUC study.[30] On the other hand, the diffusion coefficient determined by the $c(s)$ model is comparable to those by interference optics studies[44] and dynamic light scattering (DLS).[45] For examples, D values of PSSNa6 (0.10 mg/mL) in 0.010 and 0.10 M NaCl solutions measured by SV are 6.57×10^{-12} and 9.57×10^{-12} m^2/s, respectively. For PSSNa with similar molar mass (M_w = 650 000 g/mol), the D values in the corresponding NaCl solutions measured by DLS are 7.21×10^{-12} and 10.1×10^{-12} m^2/s, respectively. Thus, $c(s)$ model generally can work for the polyelectrolyte system. Typical SV analysis profiles can be found in the Supporting Information.

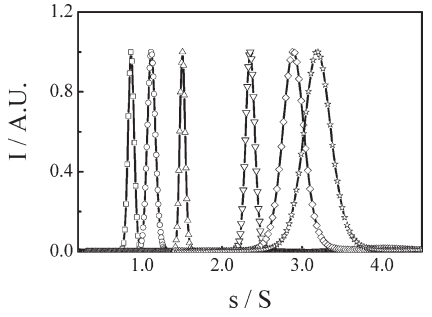

Figure 1. Sedimentation coefficient (s) distributions of PSSNa3 in NaCl solutions, where PSSNa3 concentration (C_p) is 0.10 mg/mL. From left to right, NaCl concentrations (C_s) are 0, 1.0×10^{-5}, 1.0×10^{-4}, 1.0×10^{-3}, 1.0×10^{-2}, and 0.1 M.

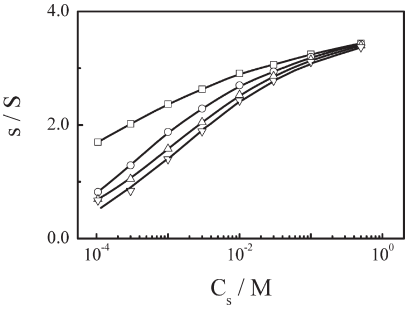

Figure 2. NaCl concentration (C_s) dependence of sedimentation coefficient (s) of PSSNa3. PSSNa3 concentrations (C_p) are 0.10 (□), 0.40 (○), 0.70 (△), and 1.0 mg/mL (▽).

The molar mass (M_w) can be obtained via the Svedberg equation. However, it is apparent since the Svedberg equation is applicable to infinite dilution solutions. The continuous $c(s,ff0)$ model was chosen to fit the polydispersity index (PDI) of a sample.[37,46] For neutral and fully screened charged solutes, relative error for s, D, or M_w is 5%.[39] For polyelectrolyte sediments in a low salt concentration solution, due to the pronounced charge effect, the obtained s, D, and M_w are apparent. As shown in Table 1, the molar masses determined by SE analyses and SV analyses are consistent, indicating the validity of SV analysis in determination of real molar mass of a polyelectrolyte. Note that as the molar mass increases, the PDI of PSSNa becomes broader than that of its precursor. This should be caused by the chain scission in the sulfonation of the polystyrene.

Salt Concentration Dependence. Figure 1 shows typical sedimentation coefficient (s) distributions of PSSNa (PSSNa3) at different salt concentrations (see Supporting Information). Clearly, s increases with C_s, indicating the charge effect on PSSNa sedimentation and chain conformation. Despite the complicated many-body problem of polyelectrolytes, we can understand their behaviors in a simple model. In a salt-free or a low salt concentration solution, each PSSNa chain can be taken to be an electrical double layer where the counterions form the diffuse layer.[47,48] While some of the counterions are condensed along the chain due to the electric attraction, the others diffuse away from the chain via thermal motion driven by osmotic pressure.[3] Thus, the electrostatic repulsion between chains or between segments in the same chain due to the effective charges is expected. Since the Debye length (r_D) (~150 nm) is larger than the separation between PSSNa chains (r_s) (~90 nm), the interchain electrostatic repulsion is long-ranged. PSSNa chains exhibit a highly extended conformation in a salt-free solution with a large hydrodynamic friction due to the interchain and intrachain repulsion. On the other hand, while the polyelectrolyte backbones sediment in centrifugal field, the small counterions disperse in solution due to their differences in molecular mass and translational speed, resulting in an electrical field which decreases the sedimentation velocity of PSSNa chains. This is the so-called primary charge effect.[49] As salt is introduced, the charged groups along the polyelectrolyte backbones are gradually screened by the counterions due to the osmotic pressure. Namely, the effective charges on the backbone decrease. However, the secondary charge effect due to the differences in mobility and molecular weight between small cations and anions also induces an electrical field, which also decreases the sedimentation velocity of the PSSNa chains.[32] Actually, polyelectrolyte behaviors are determined by hydrodynamic interactions, electrostatic interactions, and intrinsic excluded volume effect.[23,32] The long-range interchain electrostatic interaction and the hydrodynamic friction slow down the sedimentation.[49] Consequently, the added salt screens the electrostatic repulsion, and the chains become more flexible with a smaller hydrodynamic friction and s increases with C_s.[26,34,50] Note that PSSNa solution without NaCl here cannot be strictly considered to be salt-free solution since some carbonic acid can form in water during the exposure to air. The ionic strength was reported to be about 4.0×10^{-6} M.[12] Anyhow, the salt concentration is very low, and the situation is close to that for a salt-free solution. The sedimentation coefficient distribution becomes broader with increasing C_s. As discussed below, this is because s is nonlinearly related to M_w, and the difference in size of PSSNa chains is enlarged as they shrink.

On the other hand, two diffusion modes in a salt-free dilute polyelectrolyte solution were observed by DLS. The fast mode was attributed to the coupled diffusion of individual polyelectrolyte chains and the counterions,[48,51−53] while the slow mode was to temporal interchain aggregation.[54−56] Recently, by studying a polymer with charged−neutral−charged transition, Wu et al.[57] attributed the fast mode to the coupled diffusion of counterions and chains and the slow mode to the self-diffusion of the center-of-mass of individual chains caged in other surrounding chains due to the long-range electrostatic interaction. Figure 1 shows PSSNa chains in a solution with or without added salt have a unimodal distribution; only one mode was observed. However, we cannot exclude the possibility that this is because SV with concentration detector is less sensitive to large particles than DLS.

Figure 2 shows a typical salt concentration (C_s) dependence of sedimentation coefficient (s) of PSSNa sample (PSSNa3). It can be seen that s increases with C_s. As discussed above, in a salt-free or a low salt concentration solution, the interchain electrostatic repulsion and hydrodynamic friction are large, giving rise to a small sedimentation coefficient. As C_s increases, the Debye length decreases, and the interchain and intrachain electrostatic repulsions are gradually screened. The chains become more flexible and the hydrodynamic friction decreases, leading s to increase. Figure 2 also shows that for a certain C_s, s decreases with PSSNa concentration (C_p). This is because the intrinsic excluded volume effect becomes more significant with increasing C_p. We will further discuss this below.

Figure 3 shows a typical salt concentration (C_s) dependence of diffusion coefficient (D) of PSSNa sample (PSSNa3). As C_s increases, D sharply decreases and then gradually increases; that is, D exhibits a minimum. As we know, when C_s is low enough, polyelectrolyte chains adopt an extended

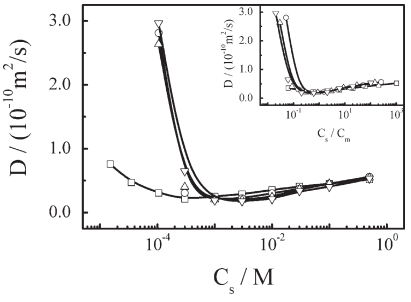

Figure 3. NaCl concentration (C_s) dependence of diffusion coefficient (D) of PSSNa3. The inset shows C_s/C_m dependence of diffusion coefficient. PSSNa concentrations (C_p) are 0.10 (□), 0.40 (○), 0.70 (△), and 1.0 mg/mL (▽).

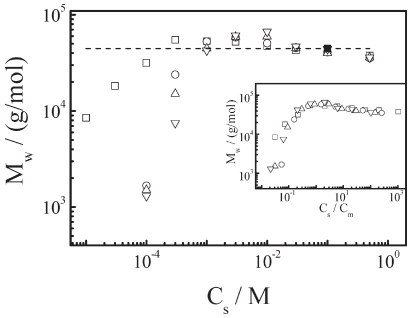

Figure 4. NaCl concentration (C_s) dependence of apparent molar mass (M_w) of PSSNa3. The inset shows C_s/C_m dependence of the apparent molar mass. The solid and open points are for SE and SV measurements, respectively. PSSNa concentration (C_p) used in SV experiments are 0.10 (□), 0.40 (○), 0.70 (△), and 1.0 mg/mL (▽). A dashed line crossing the SE result serves as a guide.

conformation, and the interchain electrostatic repulsion induced by the effective charges on the chains would accelerate their mobility at the sedimentation boundary, resulting in a large apparent diffusion coefficient.[58] As C_s increases, the effective charges and the Debye screening length decrease and the polyelectrolyte chain shrinks, leading the apparent diffusion coefficient to decrease. When the salt concentration reaches a critical value, the effective charges are almost screened completely. On the other hand, the hydrodynamic friction decreases with increasing C_s due to the chain shrinking, which increases the diffusion coefficient. The combination of the interchain electrostatic repulsion and hydrodynamic friction gives rise to the minimum. Note that the minimum also has dependence on C_p, that is, the minimum increases with C_p. To clear about it, we made a D vs C_s/C_m plot (the inset), where C_m is the monomeric unit concentration of PSSNa in mol/L (M). C_s/C_m can reflect the level of effective charges. It shows the minimum does not have dependence on C_s/C_m. The C_s/C_m value corresponding to the minimum is about 0.2−0.5. Actually, the minimum also does not vary with the molar mass of PSSNa (data not shown). The facts clearly indicate that the interchain electrostatic repulsion from the effective charges greatly influences the diffusion at a low salt concentration.

Figure 4 shows the salt concentration dependence of the apparent molar mass (M_w) of PSSNa sample (PSSNa3). As stated above, when C_s is lower than $\sim 1.0 \times 10^{-3}$ M, the electrostatic repulsion induces low sedimentation coefficient and high diffusion coefficient, so we obtained an underestimated molar mass based on eq 4. As C_s increases, the electrostatic repulsion is gradually screened so that the apparent molar mass increases. When C_s reaches $\sim 1.0 \times 10^{-3}$ M, M_w is almost a constant and close to that measured by SE. Since SE measurement gives the absolute molar mass

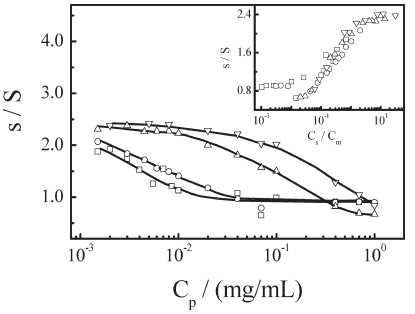

Figure 5. PSSNa3 concentration (C_p) dependence of sedimentation coefficient (s). The inset shows C_s/C_m dependence of sedimentation coefficient (s). NaCl concentrations (C_s) are 0 (□), 1.0×10^{-5} (○), 1.0×10^{-4} (△), and 3.0×10^{-4} M (▽).

with a high accuracy, the present results indicate that SV with SEDFIT analysis can be used to determine the real molar mass of polyelectrolytes when C_s is high enough. This can be viewed more clearly from the C_s/C_m dependence of apparent molar mass (M_w) in the inset. It shows that M_w is invariant when C_s/C_m is higher than 0.2−0.5, consistent with the results in Figure 3. This is an indication that the interchain electrostatic repulsion is suppressed there. Furthermore, the apparent molar mass does not increase with NaCl concentration, indicating the conformational change of individual chains.

Polyelectrolyte Concentration Dependence. The effects of polyelectrolyte concentration on its dynamics are complex. First, we focus on the case with a low NaCl concentration. Figure 5 shows PSSNa3 concentration (C_p) dependence of sedimentation coefficient (s) when NaCl concentration (C_s) is lower than 3.0×10^{-4} M. Generally, s decreases with increasing C_p at each salt concentration. However, the salt concentration also influences the sedimentation coefficient. In a solution without added salt or a low salt solution, s quickly decreases and then levels off as C_p increases. In contrast, when C_s is above 1.0×10^{-4} M, s slightly varies in a certain range of C_p. It drops to a constant when C_p reaches a critical value. Moreover, the initial plateau becomes broader as NaCl concentration increases. As we know, in a very dilute solution without added salt, the chains together with their diffuse layers separate far away, and the counterions are condensed along each polyelectrolyte backbone or freely move around the chain. The interchain interactions including hydrodynamic interactions, electrostatic interactions, and intrinsic excluded volume effect are relatively weak. As C_p increases, the separation between the chains becomes so narrow that the neighboring chains can share the mobile counterions each other, which allows the chains to correlate each other. Though the interchain electrostatic repulsion is still weak when $C_p < 0.010$ mg/mL because the chain separation (~200 nm) is larger than the Debye length (~150 nm), the hydrodynamic interactions between the chains increase, leading the sedimentation coefficient to decrease. Further increasing C_p also leads to the interchain electrostatic repulsion, which further reduces the sedimentation coefficient. It is known that the counterion condensation is the interplay between the electrostatic attraction of the polyelectrolyte chain to the small counterions and the entropic loss of counterions when they are localized near the polyelectrolyte chain.[3] When C_p is above a critical value, the counterion condensation reaches equilibrium. Thus, the interchain electrostatic repulsion and hydrodynamic interactions slightly vary with C_p, and s almost holds a constant.

In a higher salt solution, the mobile counterions are enough to induce the interchain interactions. However, the

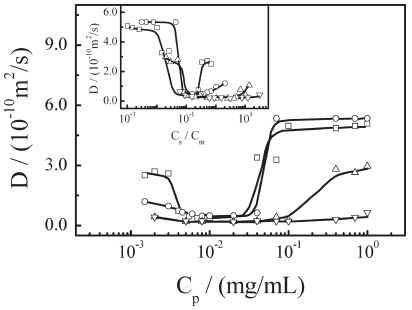

Figure 6. PSSNa3 concentration (C_p) dependence of diffusion coefficient (D). The inset shows C_s/C_m dependence of diffusion coefficient (D). NaCl concentrations (C_s) are 0 (□), 1.0×10^{-5} (○), 1.0×10^{-4} (△), and 3.0×10^{-4} M (▽).

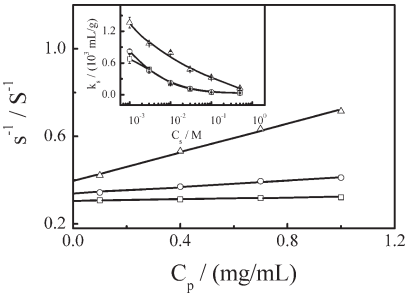

Figure 7. PSSNa3 concentration (C_p) dependence of reciprocal sedimentation coefficient (s^{-1}) in NaCl solutions, where NaCl concentrations are 1.0×10^{-3} (△), 1.0×10^{-2} (○), and 0.10 M (□). The inset shows C_s dependence of k_s for PSSNa1 (□), PSSNa3 (○), and PSSNa6 (△).

mobile counterions from polyelectrolyte chains are limited in comparison with those from the added salt, so that the interchain interactions slightly increase with C_p. When C_p is above a critical value, the former become dominant, and the interchain interactions markedly increase with C_p. As a result, s slightly changes in a certain C_p range before a drop. Clearly, such a C_p range becomes broader as the salt concentration increases. Further increasing C_p leads the counterion condensation to reach equilibrium, and s no longer varies. Figure 5 also shows that s increases with the salt concentration. This is because the interchain electrostatic repulsion decreases with salt concentration.

Figure 6 shows PSSNa3 concentration (C_p) dependence of the apparent diffusion coefficient (D) when salt concentration (C_s) is lower than 3.0×10^{-4} M. In a solution without added salt, the apparent diffusion coefficient first decreases and then increases with increasing C_p; namely, D exhibits a minimum. As discussed above, the chain separation is larger than the Debye length in a very dilute solution ($C_p < \sim 0.005$ mg/mL for PSSNa3); the polyelectrolyte chains almost do not interact with each other. The chains can move very freely with a relatively large diffusion coefficient. Note that the ionic strength increases with polyelectrolyte concentration because the counterion concentration increases. However, because of the counterion condensation, such an increase is small so that it would lead to a limited shrinking of the polyelectrolyte chains. When C_p is above ~0.005 mg/mL, the separation between the chains is short enough; the hydrodynamic interactions between the chains increase, leading the diffusion coefficient to decrease. The interchain electrostatic repulsion is still weak in this range because the chain separation is larger than the Debye length. In the C_p range of ~0.010 to ~0.030 mg/mL, both interchain electrostatic repulsion and hydrodynamic friction increase with increasing C_p; their combination leads the apparent diffusion coefficient to vary slightly. When C_p is above ~0.030 mg/mL, the chain separation (~140 nm) is comparable with the Debye length (~150 nm), giving rise to the interchain electrostatic repulsion, which accelerates the boundary diffusion. Budd[34] observed a larger diffusion coefficient of PSSNa ($M_w = 1.06 \times 10^6$ g/mol) at high PSSNa concentration in a salt-free solution by AUC and demonstrated that it corresponds to the fast mode in DLS. Moreover, such a fast mode does not have molar mass dependence.[34,54] Clearly, our results agree with Budd's.

Further increasing C_p leads to the interchain electrostatic repulsion, so both the counterion condensation and hydrodynamic friction increase. Their combination leads the apparent diffusion coefficient to level off. A similar phenomenon is also observed in a solution with a low NaCl concentration. However, because the counterion condensation also increases with NaCl concentration, the change in the apparent diffusion coefficient as a function of C_p becomes less pronounced with increasing NaCl concentration. The minimum diffusion coefficient results from the interchain interactions related to chain−chain separation and counterion condensation. Note that we did not observe an extremum for the sedimentation coefficient in Figures 2 and 5. This is probably because the interchain interactions have much more pronounced effects on the diffusion coefficient than the sedimentation coefficient.

It was reported that diluting a polyelectrolyte solution leads to a nonmonotonical variation of reduced viscosity.[12,59] The maximum reduced viscosity locates at about 0.005 mg/mL in salt-free solution, and the location does not have molar mass dependence. These agree well with the results about the minimum diffusion coefficient here. On the other hand, as the concentration of added salt increases, the magnitude of maximum reduced viscosity decreases but it always locates at $C_s/C_m = 0.25$.[12,59] The inset of Figure 6 shows that the location of minimum diffusion coefficient for each sample covers a range of C_s/C_m from 0.2 to 0.5. This generally agrees with that for the maximum reduced viscosity. Since diffusion coefficient (D) relates to viscosity (η) or hydrodynamic volume, the present study further indicates that the maximum reduced viscosity is the result of interchain electrostatic repulsion and hydrodynamic interactions.[12,23]

Now, let us turn to the case with a higher NaCl concentration. Figure 7 shows that s linearly decrease as C_p increases when C_s is above 1.0×10^{-3} M. As discussed above, the interchain electrostatic repulsion is suppressed in this range. Because the hydrodynamic friction and intrinsic excluded volume effect become more pronounced as C_p increases, the sedimentation slows down. Extrapolation of s to zero PSSNa concentration leads to the sedimentation coefficient (s_0) at infinite dilution, which can be taken as the sedimentation coefficient of a single chain without interchain interactions. For each sample, we have $s^{-1} = s_0{}^{-1}(1 + k_s C_p + ...)$, where k_s is the sedimentation concentration coefficient. k_s can reflect the interactions between chains.[60,61] The inset shows k_s increases with molar mass but decreases with salt concentration, indicating that chains with higher molar mass interact with each other more strongly, and the added salt reduces the interchain interactions.

Figure 8 shows D linearly decreases with C_p when C_s is above 1.0×10^{-3} M, where the interchain electrostatic repulsion is suppressed. This is because the hydrodynamic friction and intrinsic excluded volume effect increase with C_p and reduce the diffusion coefficient. By extrapolating D to zero concentration, we obtain the diffusion coefficient D_0 at infinite dilution or the diffusion coefficient of a single chain without interchain interactions. Clearly, we have $D = D_0(1 + k_D C_p + ...)$,

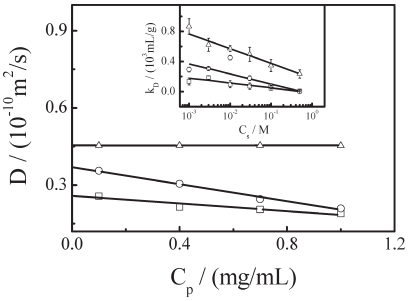

Figure 8. PSSNa3 concentration (C_p) dependence of diffusion coefficient (D) in NaCl solutions, where NaCl concentrations (C_s) are 1.0×10^{-3} (□), 1.0×10^{-2} (○), and 0.10 M (△). The inset shows C_s dependence of k_D for PSSNa1 (□), PSSNa3 (○), and PSSNa6 (△).

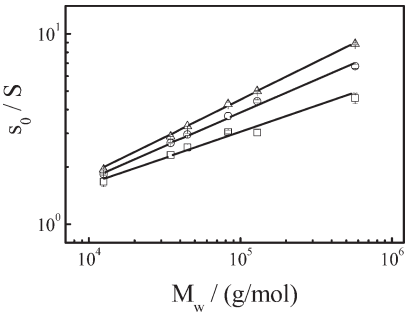

Figure 9. Molar mass (M_w) dependence of PSSNa sedimentation coefficient (s_0) at infinite dilution in NaCl solutions, where NaCl concentrations (C_s) are 1.0×10^{-3} (□), 1.0×10^{-2} (○), and 0.10 M (△).

where k_D is the diffusion concentration coefficient.[61] Like k_s, k_D is a measure of interchain interactions. The inset shows that k_D increases with the molar mass of PSSNa and decreases with salt concentration. Note that k_D does not monotonically decrease with salt concentration. This is probably because the diffusion coefficient has some concentration dependence, which is not considered by SEDFIT.

Molar Mass Dependence of Sedimentation Coefficient or Diffusion Coefficient. The scaling relations between real molar mass and sedimentation coefficient or diffusion coefficient can be used to characterize the chain conformation change.[40,62,63] Figure 9 shows the molar mass (M_w) dependence of sedimentation coefficient (s_0) at infinite dilution in a double-logarithmic plot. Since the sedimentation coefficient is nonlinearly related to the polyelectrolyte concentration at low salt concentration, we only considered the cases when C_s is higher than 1.0×10^{-3} M. It is known that $s = (1 - \nu\rho_0)M_w/f$ based on eqs 4 and 5; that is, sedimentation coefficient increases with molar mass of a polymer but decreases with the hydrodynamic friction. Since the former dominates the latter here, it is reasonable that s_0 increases with M_w. On the other hand, Figure 10 shows that D_0 decreases with M_w. This is because the hydrodynamic friction increases with the molar mass of the polyelectrolytes.

It is known that for a polymer s and D scale to M_w as[64]

$$s_0 = K_s M_w^{\alpha} \quad (7)$$

$$D_0 = K_D M_w^{-\beta} \quad (8)$$

where s_0 and D_0 are the sedimentation coefficient and diffusion coefficient of the polymer at infinite dilution. K_s and K_D are the scaling prefactors. α and β are the scaling indexes. In addition, $\alpha + \beta = 1$ in terms of eqs 4−8. From Figures 9 and 10, we have

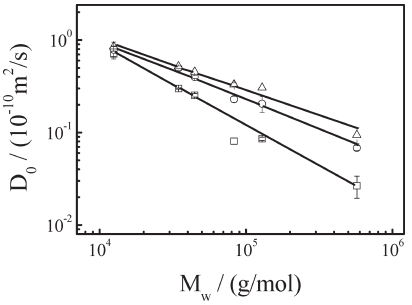

Figure 10. Molar mass (M_w) dependence of PSSNa diffusion coefficient (D_0) at infinite dilution in NaCl solutions, where NaCl concentrations (C_s) are 1.0×10^{-3} (□), 1.0×10^{-2} (○), and 0.10 M (△).

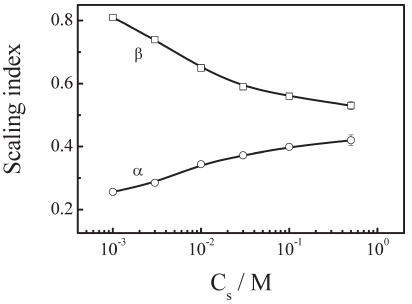

Figure 11. NaCl concentration (C_s) dependence of the scaling indexes.

$s_0 = K_s M_w^{\alpha}$ and $D_0 = K_D M_w^{-\beta}$. The scaling indexes can give the information about the chain conformation. For a rigid rod, $\alpha = 0.15$ and $\beta = 0.85$. For a random coil $\alpha = 0.4-0.5$ and $\beta = 0.5-0.6$. For a compact sphere, $\alpha = 0.67$ and $\beta = 0.33$.[64] Figure 11 shows that α increases but β deceases as C_s increases, clearly indicating the shrinking of the PSSNa chains. When C_s is 1.0×10^{-3} M, α and β are 0.26 and 0.81, respectively, indicating that the PSSNa chains adopt a semirigid chain conformation. This is because the charges still interact through the unscreened Coulomb potential at a distance much smaller than the Debye screening length even when interchain repulsion is screened. The intrachain repulsion allows the polyelectrolyte chains to have certain stiffness, and they are flexible on large length scales.[3] PSSNa chains are expected to be more extended in a lower salt concentration solution and the most extended in a salt-free solution though we were not able to obtain the α and β values when C_s is lower than 1.0×10^{-3} M. As C_s increases over 3.0×10^{-2} M, $\alpha = 0.4-0.5$ and $\beta = 0.5-0.6$, indicating that PSSNa chains change into random coils. Note that $\alpha = 0.42$ and $\beta = 0.55$ even at the highest salt concentration ($C_s = 0.50$ M) in the range we investigated, indicating that NaCl solution is still a good solvent for PSSNa.[64] The salt concentration dependence of α and β indicates that PSSNa chains shrink from a highly extended conformation to a coil as NaCl concentration increases. Clearly, the conformational change is mediated by the electrostatic interactions, hydrodynamic interactions, and intrinsic excluded volume effect.[23]

Conclusion

In conclusion, we have systematically investigated the sedimentation and diffusion of poly(sodium styrenesulfonate) (PSSNa) with different molar mass in aqueous solutions with and without NaCl by use of an analytical ultracentrifuge (AUC) via sedimentation velocity (SV) analysis. SV analysis is an efficient method to determine sedimentation coefficient, diffusion coefficient, and molar mass of polyelectrolytes. As salt concentration increases, the sedimentation coefficient increases, whereas the diffusion

coefficient exhibits a minimum. On the other hand, at a low salt concentration, the sedimentation coefficient decreases whereas the diffusion coefficient exhibits a minimum as the polyelectrolyte concentration increases. At a higher salt concentration, the sedimentation coefficient or diffusion coefficient is linearly related to the polyelectrolyte concentration. The scaling relation between molar mass and sedimentation coefficient or diffusion coefficient indicates the chain shrinks from extended rod to random coil. The dynamics of polyelectrolyte chains is mediated by the electrostatic interactions, hydrodynamic interactions, and intrinsic excluded volume effect.

Acknowledgment. The financial support of the National Distinguished Young Investigator Fund (20725414) and Ministry of Science and Technology of China (2007CB936401) is acknowledged. We thank Dr. P. Schuck from the NIH for the valuable discussions.

Supporting Information Available: Sedimentation coefficients by $c(s)$ model and Transport model, SE data analysis, SV data analysis, and the sedimentation coefficient distributions. This material is available free of charge via the Internet at http://pubs.acs.org.

References and Notes

(1) Nalwa, H. S. *Handbook of Polyelectrolytes and Their Applications*; American Scientific Publishers: Stevenson Ranch, CA, 2002.
(2) Forster, S.; Schmidt, M. *Adv. Polym. Sci.* **1995**, *120*, 51–133.
(3) Dobrynin, A. V.; Rubinstein, M. *Prog. Polym. Sci.* **2005**, *30*, 1049–1118.
(4) Holm, C.; Joanny, J. F.; Kremer, K.; Netz, R. R.; Reineker, P.; Seidel, C.; Vilgis, T. A.; Winkler, R. G. *Adv. Polym. Sci.* **2004**, *166*, 3–17.
(5) Oosawa, F. *Polyelectrolytes*; Marcel Dekker: New York, 1971.
(6) Manning, G. S. *J. Chem. Phys.* **1969**, *51*, 924933.
(7) Raphael, E.; Joanny, J. F. *Europhys. Lett.* **1990**, *13*, 623–628.
(8) Muthukumar, M. *J. Chem. Phys.* **2004**, *120*, 9343–9350.
(9) Odijk, T. *J. Polym. Sci., Polym. Phys. Ed.* **1977**, *15*, 477–483.
(10) Skolnick, J.; Fixman, M. *Macromolecules* **1977**, *10*, 944–948.
(11) Fixman, M. *J. Phys. Chem. B* **2010**, *114*, 3185–3196.
(12) Cohen, J.; Priel, Z.; Rabin, Y. *J. Chem. Phys.* **1988**, *88*, 7111–7116.
(13) Yamanaka, J.; Matsuoka, H.; Kitano, H.; Hasegawa, M.; Ise, N. *J. Am. Chem. Soc.* **1990**, *112*, 587–592.
(14) Wignall, G. D.; Melnichenko, Y. B. *Rep. Prog. Phys.* **2005**, *68*, 1761–1810.
(15) Spiteri, M. N.; Williams, C. E.; Boue, F. *Macromolecules* **2007**, *40*, 6679–6691.
(16) Schweins, R.; Huber, K. *Eur. Phys. J. E* **2001**, *5*, 117–126.
(17) Amis, E. J.; Valachovic, D. E.; Sedlak, M. *ACS Symp. Ser.* **1994**, *548*, 322–336.
(18) Volk, N.; Vollmer, D.; Schmidt, M.; Oppermann, W.; Huber, K. *Adv. Polym. Sci.* **2004**, *166*, 29–65.
(19) Koene, R. S.; Mandel, M. *Macromolecules* **1983**, *16*, 973–978.
(20) Katchalsky, A.; Künzle, O.; Kuhn, W. *J. Polym. Sci.* **1950**, *5*, 283–300.
(21) Lifson, S. *J. Polym. Sci.* **1957**, *23*, 431–442.
(22) Alexandrowicz, Z. *J. Chem. Phys.* **1967**, *47*, 4377–4384.
(23) Ashok, B.; Muthukumar, M. *J. Phys. Chem. B* **2009**, *113*, 5736–5745.
(24) Takahashi, A.; Kato, T.; Nagasawa, M. *J. Phys. Chem.* **1967**, *71*, 2001–2010.
(25) Laue, T. M.; Stafford, W. F. *Annu. Rev. Biophys. Biomol. Struct.* **1999**, *28*, 75–100.
(26) Mächtle, W.; Börger, L. *Analytical Ultracentrifugation of Polymers and Nanoparticles*; Springer: Berlin, 2006.
(27) Wagner, M.; Oppermann, W. *Proceedings of Yamada Conference L Polyelectrolytes*; Yamada Science Foundation: Osaka, 1999; pp 100−103.
(28) Harding, S. E. *Adv. Polym. Sci.* **2005**, *186*, 211–254.
(29) Budd, P. M. *Br. Polym. J.* **1988**, *20*, 33–37.
(30) Budd, P. M. *Polymer* **1985**, *26*, 1519–1522.
(31) Pavlov, G. M.; Zaitseva II; Guintrinsicv, A. S.; Korneeva, E. V.; Gavrilova II; Panarin, E. F. *Dokl. Chem.* **2008**, *419*, 111–112.
(32) Inagaki, H.; Hotta, S.; Hirami, M. *Makromol. Chem.* **1957**, *23*, 1–15.
(33) Nagasawa, M.; Eguchi, Y. *J. Phys. Chem.* **1967**, *71*, 880–888.
(34) Budd, P. M. *Prog. Colloid Polym. Sci.* **1994**, *94*, 107–115.
(35) Budd, P. M. *Analytical Ultracentrifugation in Biochemistry and Polymer Science*; Royal Society of Chemistry: London, 1992; pp 593−608.
(36) Lebowitz, J.; Lewis, M. S.; Schuck, P. *Protein Sci.* **2002**, *11*, 2067–2079.
(37) Schuck, P. *Biophys. J.* **1998**, *75*, 1503–1512.
(38) Vistica, J.; Dam, J.; Balbo, A.; Yikilmaz, E.; Mariuzza, R. A.; Rouault, T. A.; Schuck, P. *Anal. Biochem.* **2004**, *326*, 234–256.
(39) Cole, J. L.; Lary, J. W.; P. Moody, T. P.; Laue, T. M. *Methods Cell Biol.* **2008**, *84*, 143–179.
(40) Dobrynin, A. V.; Colby, R. H.; Rubinstein, M. *Macromolecules* **1995**, *28*, 1859–1871.
(41) Boris, D. C.; Colby, R. H. *Macromolecules* **1998**, *31*, 5746–5755.
(42) Philo, J. S. *Anal. Biochem.* **2006**, *354*, 238–246.
(43) Dam, J.; Schuck, P. *Method Enzymol.* **2004**, *384*, 185–212.
(44) Suzuki, Y.; Noda, I.; Nagasawa, M. *J. Phys. Chem.* **1969**, *73*, 797–803.
(45) Koene, R. S.; Nicolai, T.; Mandel, M. *Macromolecules* **1983**, *16*, 227–231.
(46) Brown, P. H.; Schuck, P. *Biophys. J.* **2006**, *90*, 4651–4661.
(47) Muthukumar, M. *J. Chem. Phys.* **1987**, *86*, 7230–7235.
(48) Muthukumar, M. *J. Chem. Phys.* **1996**, *105*, 5183–5199.
(49) Pedersen, K. O. *J. Phys. Chem.* **1958**, *62*, 1282–1290.
(50) Kumar, R.; Kundagrami, A.; Muthukumar, M. *Macromolecules* **2009**, *42*, 1370–1379.
(51) Muthukumar, M. *J. Chem. Phys.* **1997**, *107*, 2619–2635.
(52) Muthukumar, M. *Adv. Chem. Phys.* **2005**, *131*, 1–60.
(53) Lin, S. C.; Lee, W. I.; Schurr, J. M. *Biopolymers* **1978**, *17*, 1041–1064.
(54) Sedlak, M.; Amis, E. J. *J. Chem. Phys.* **1992**, *96*, 817–825.
(55) Ermi, B. D.; Amis, E. J. *Macromolecules* **1998**, *31*, 7378–7384.
(56) Cong, R. J.; Temyanko, E.; Russo, P. S.; Edwin, N.; Uppu, R. M. *Macromolecules* **2006**, *39*, 731–739.
(57) Zhou, K.; Li, J.; Lu, Y.; Zhang, G.; Xie, Z.; Wu, C. *Macromolecules* **2009**, *42*, 7146–7154.
(58) Varoqui, R.; Schmitt, A. *Biopolymers* **1972**, *11*, 1119–1136.
(59) Fuoss, R. M.; Strauss, U. P. *J. Polym. Sci.* **1948**, *3*, 602–603.
(60) Rowe, A. J. *Biopolymers* **1977**, *16*, 2595–2611.
(61) Solovyova, A.; Schuck, P.; Costenaro, L.; Ebel, C. *Biophys. J.* **2001**, *81*, 1868–1880.
(62) de Gennes, P. G.; Pincus, P.; Velasco, R. M.; Brochard, F. *J. Phys. (Paris)* **1976**, *37*, 1461–1473.
(63) Pfeuty, P. *J. Phys., Colloq.* **1978**, *39*, C2−149–C2−160.
(64) Harding, S. E. *Biophys. Chem.* **1995**, *55*, 69–93.